FAULT DETECTION FILTER APPLIED TO STRUCTURAL HEALTH MONITORING: EXPERIMENTAL RESULTS

Sauro Liberatore * **Jason L. Speyer** *
Andy Chunliang Hsu *

* *Mechanical and Aerospace Engineering Department, UCLA*

Abstract: A model based fault detection filter is developed for structural health monitoring of a simply supported beam. The structural damage represented in the plant model is decomposed and is shown to reduce to a fault direction vector maintaining a fixed direction. According to detection filter theory, this fault detection vector under certain circumstances can be uniquely detected and identified through an invariance in the direction imposed on the fault detection filter residuals. The design algorithm uses a left eigenstructure assignment approach. The filter is applied to data from an aluminum simply supported beam with 4 piezoelectric sensors and 1 piezoelectric actuator. By exciting the structure at the first natural frequency, a 5 mm saw cut made to one side of the beam, is detected and localized.

Keywords: Fault detection and identification, health monitoring, structural health monitoring, fault location

1. INTRODUCTION

The ability to detect a system fault at the earliest possible stage is of primary interest in the operation of highly reliable system. A system that continuously monitors a structure in order to detect damage, is often referred to as a health monitoring system. The system based on detection filters is constructed to detect and identify the fault rapidly. In our approach the system dynamics are modelled to construct a filter which generates a residual as the difference between system measurements and the estimated system measurements. The fault detection filter gains are designed to have the filter residual in an invariant direction in the presence of an element from a set of *a priori* known faults which allows both detection and identification.

[1] This work was supported by AFOSR Grant No. F49620-02-1-0139.

The fault detection filter was first introduced by (Beard, 1971) and refined by (Jones, 1973) and is also known as Beard–Jones detection filter. A spectral analysis of the Beard–Jones detection filter and an associated algorithm have been developed in (White and Speyer, 1987). A generalization of the Beard–Jones detection filter has been developed in (Massoumnia, 1986), called the restricted diagonal detection filter (Massoumnia, 1986). An algorithm that implements the restricted diagonal detection filter is based on the spectral method developed by (Douglas and Speyer, 1996; Douglas and Speyer, 1999). This approach to detection filter design was implemented here for two reasons. First, a filter that could process the many faults needed for the structural damage detection is desirable. Secondly, this procedure is used because it can hedge against sensitivity to parameter uncertainty. Since there might be many fault directions placed in a single detection filter, the sensitivity of the filter

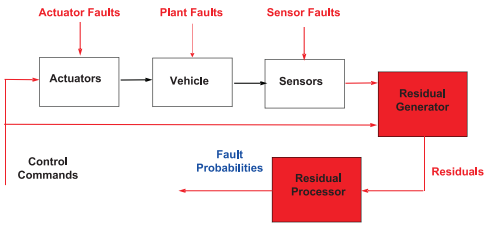

Fig. 1. Fault detection and identification

to the fault directions can be assessed by the ill-conditioning in the gain calculations (Douglas and Speyer, 1996). Directions that produce ill-conditioning can be removed for the purposes of detection (a target fault), but can be retained to ensure that if it occurs, it will not appear in the filter residual (a nuisance fault). Since the gains are not unique, filter robustness tradeoffs between filter sensitivity and process and measurement noise rejection can be addressed by the approach given in (Douglas and Speyer, 1996). However, it was felt that sensitivity to the fault directions were the dominant uncertainty, although some robustness trades were made by the choice of the filter eigenvalues and the eigenvectors associated with the complementary subspace.

The proposed health monitoring system, shown in Figure 1, consists of these two components: residual generator and residual processor. In the first stage, the residual generator uses the control commands and measurements to generate the residual. In the second stage, the residual processor uses the residual to generate the probability of each fault hypothesis (Malladi and Speyer, 1999). Only the development and experimental evaluation of the fault detection filter is given here.

In section 4, the filter is applied to the detection and identification of structural faults in a simply supported beam. The measurements and actuation of the beam are obtained from piezoelectric transducers that ensure a large operating bandwidth. The algorithm is specifically accomplished by using 4 sensors and 1 actuator and relies on a mathematical model of the structure.

In addition to structural faults, the fault detection filter method could include sensors and actuator faults even if, in the present paper, only structural faults are considered.

2. FAULT DETECTION FILTER

Consider a linear time invariant system

$$\dot{x} = \mathbf{A}x + \mathbf{B}u, \qquad y = \mathbf{C}x \tag{1}$$

where $\mathbf{A}$, $\mathbf{B}$ and $\mathbf{C}$ are matrices, u is the input and y is the measurement. Suppose that q failure modes occur in the system. Then, the state equation including the faults are written as

$$\dot{x} = \mathbf{A}x + \mathbf{B}u + \sum_{i=1}^{q} F_i \mu_i, \quad y = \mathbf{C}x \tag{2}$$

where F_i are assumed known fault direction vectors related to each fault and μ_i (failure magnitudes) are unknown arbitrary time functions. We assume that F_i are monic, so that $\mu_i \neq 0$ implies that $F_i\mu_i \neq 0$. Equation (2) represents the manner that plant and actuator faults enter a system. To include sensor faults in this form, a simple transformation is required (see (White and Speyer, 1987)). The fault detection filter is a linear observer

$$\dot{\hat{x}} = \mathbf{A}\hat{x} + \mathbf{B}u + \mathbf{L}r, \quad r = (y - \mathbf{C}\hat{x}) \tag{3}$$

where the gain $\mathbf{L}$ is to be chosen so that the residual, r defined as the difference between the true measurement, y and the estimate measurement $\hat{x}$ has a unique directional behavior for each particular fault. Subsequently, by defining the error between true state, x, and estimated state, $\hat{x}$, $e = (x - \hat{x})$, from Equations (2) and (3), the error system dynamic equation is obtained as

$$\dot{e} = (\mathbf{A} - \mathbf{LC})e + \sum_{i=1}^{q} F_i \mu_i, \quad r = \mathbf{C}e\,. \tag{4}$$

If the observer gains $\mathbf{L}$ are chosen such that $(\mathbf{A} - \mathbf{LC})$ is stable and if $(\mathbf{C}, \mathbf{A})$ is observable, then after a transient response and in absence of disturbances, the steady state residual r is nonzero only if μ_i are different from zero. Therefore, any stable observer can detect the fault by monitoring the residual. A more difficult task is to determine which of the q faults has occurred. The fault detection filter is capable to distinguish among them. The idea is to define the filter gains $\mathbf{L}$ such that the error e remains in an invariant subspace when the fault occurs. These subspaces must not overlap each other in order to guarantee the identification of the fault. The invariance of the subspaces with the condition given as follows, implies that the residual r has fixed directions. In order to isolate the faults, projectors $\mathbf{H}_i$ are designed such that the projected residual $(R_i = \mathbf{H}_i r)$ is sensitive only to the i-th fault.

2.1 Residual Projectors

In the previous section, we have introduced the projectors $\mathbf{H}_i$ such that the projected residuals $R_i = \mathbf{H}_i r$ annihilate all the faults except the i-th. The procedure for the design of such operators is described next. Assume that there are n fault direction vectors and F_i is the fault to be identified. Let us define the following matrix $\hat{\mathbf{F}}_i = [F_1,\ F_2, \ldots F_{i-1}, \ldots F_{i+1}, F_n]$ that collect column-wise all the faults except the i-th. By

defining the following matrices, $\mathbf{\Gamma}_i = \mathbf{C}\mathbf{A}^{\delta}\hat{\mathbf{F}}_i$ [2] the projectors are constructed as

$$\mathbf{H}_i = \mathbf{I} - \mathbf{\Gamma}_i \left[\mathbf{\Gamma}_i^T \mathbf{\Gamma}_i\right]^{-1} \mathbf{\Gamma}_i \,.$$

3. SIMPLY SUPPORTED BEAM

The structure is an aluminum simply supported beam of rectangular cross section with a piezoelectric actuator placed on the bottom of the beam surface and piezoelectric sensors placed on the beam top surface, as shown in Figure2. The reference frame is taken from the center of the cross section such that the x-axis coincides with the beam neutral axis. The analysis is limited to the bending behavior of the structure with small deformations. The Euler–Bernouilli hypothesis are assumed of plane sections that rotate because of bending and remain planer after deformation (Géradin and Rixen, 1997). The beam's potential and kinetic energy are expressed in terms of vertical displacements, $w(x,t)$, (Géradin and Rixen, 1997) and are functions of the structure Young's Modulus and mass density, respectively. When damage is present, different expressions for the beam's potential and kinetic energy are necessary. In order to represent a crack-type damage, a region of the structure is modelled such that the beam's potential and kinetic energy has different stiffness (Young's Modulus) when compared with the undamaged structure (see Figure 2). The mass density of damaged region is assumed

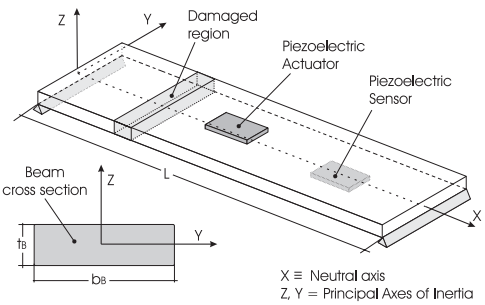

Fig. 2. Scheme of the simply supported beam. Included are the damaged region, one piezoelectric sensor and one piezoelectric actuator

unchanged because of the negligible mass reduction consequent to a crack. The displacements across the undamaged-damaged-undamaged interfaces are assumed continuous. With these assumptions, the kinetic energy, remains unchanged while the volume integral of the potential energy needs to be partitioned because the Young's Modulus is not constant along the structure length.

For the piezoelectric actuator, in addition to strain energy, the potential energy must include the contribution of the electrical field (Parton and Kudryavtsev, 1988). It is assumed that the piezoelectric transducer is polarized in the thickness direction and undergoes only longitudinal deformations. The kinetic energy for the actuator and sensors are included in the model. Given the small electric field experienced in the piezoelectric sensor, the electrical terms can be neglected and only strain energy contributes to the potential energy.

The equation of motion are obtained by applying the Rayleigh–Ritz method (Géradin and Rixen, 1997), which approximates the unknown displacements $w(x,t)$ with the series of sinusoidal shape functions

$$\begin{aligned} w(x,t) &= \sum_{j=1}^{q} B_j(t) \sin\left(\frac{j\pi x}{L}\right) \\ &= \sum_{j=1}^{q} B_j(t) \sin(k_j x) \end{aligned} \tag{5}$$

which are required to satisfy the natural boundary condition for the simply supported beam, i.e., $w(0,t) = w(L,t) = 0$. Upon substitution of Equation (5), the potential and kinetic energy are expressed in terms of the series expansion coefficients $B_j(t)$. The system *Lagrangian*, $\mathcal{L}\left(B_j(t), \dot{B}_j(t), t\right) = T_{\text{Tot}} - P_{\text{Tot}}$ ($T_{\text{Tot}} \sim$ total kinetic energy, $P_{\text{Tot}} \sim$ total potential energy), is thereby obtained by collecting the energy expressions of the sensor, actuator and beam. By means of *Lagrange's Equations*, the *Lagrangian* provides the equation of motion

$$\mathbf{M}\ddot{X}(t) + \mathbf{K}X(t) = Q \tag{6}$$

where $X(t) = \{B_1, B_2, \ldots, B_q\}^T$ is the generalized vector, $\mathbf{M}$ and $\mathbf{K}$ are the generalized mass and stiffness matrices, respectively and Q is the generalized forcing terms. In the equation of motion, damping is included by means of modal coefficients, ξ_j, whose values are evaluated based on the experimental measurements, (Gatti and Ferrari, 1999), $\mathbf{D} = \mathbf{M}\Phi\Lambda\Phi^T\mathbf{M}$ where the diagonal matric $\Lambda = \text{diag}[2\xi_j\omega_j]$, ω_j are the system natural frequencies and the matrix Φ is obtained with the system eigenvectors ordered column-wise $\Phi = [\phi_1, \phi_2, \ldots, \phi_n]$. The equation of motion can be written in its final form

$$\mathbf{M}\ddot{X}(t) + \mathbf{D}\dot{X}(t) + \mathbf{K}X(t) = Q \tag{7}$$

3.1 State-variable description

The equation of motion (7), is rearranged in a linear time invariant state space form

$$\dot{\zeta}(t) = \mathbf{A}\zeta(t) + \mathbf{B}\Delta\phi_A, \quad X(t) = \mathbf{C}^*\zeta(t) \tag{8}$$

where the state vector is defined by means of the generalized displacement vector $\zeta(t) =$

[2] δ is the smallest integer such that $\mathbf{C}\mathbf{A}^{\delta}F_i \neq 0$. For our system, $\delta = 1$

$\{X(t), \dot{X}(t)\}^T$, $\Delta\phi_A$ is the voltage input applied to the actuator and $\mathbf{A}$, $\mathbf{B}$ and $\mathbf{C}^*$ are defined as follows

$$\mathbf{A} = \begin{bmatrix} \mathbf{0} & \mathbf{I} \\ -\mathbf{M}^{-1}\mathbf{K} & -\mathbf{M}^{-1}\mathbf{D} \end{bmatrix}, \quad \mathbf{B} = \begin{Bmatrix} 0 \\ Q^* \end{Bmatrix} \quad (9)$$
$$\mathbf{C}^* = [\mathbf{I}, \mathbf{0}], \qquad Q^*\Delta\Phi_A = Q\,.$$

The output from Equation (8) is the generalized displacement vector, whose components are the coefficients of the series expansion, Equation (5).

The output voltage from each sensor is proportional to the strains. Because this voltage is generally very small, the hypothesis of *zero flux*, (Parton and Kudryavtsev, 1988), can be utilized. $\Delta\phi_{Si}$ are the voltage outputs of each sensor and are related to the state vectors ζ (Liberatore, 2002). The final form of the dynamic system is

$$\dot{\zeta}(t) = \mathbf{A}\zeta(t) + \mathbf{B}\Delta\phi_A, \quad \Delta\phi_S = \mathbf{C}\zeta(t)\,. \quad (10)$$

3.2 Fault decomposition

Structural damage is included in the $\mathbf{A}$ matrix (Equation (9)), as $\bar{\mathbf{A}} = (\mathbf{A} + \delta\mathbf{A})$, where $\delta\mathbf{A}$ is partitioned into four blocks having three zero blocks and the lower left block being $-\mathbf{M}^{-1}\delta\mathbf{K}$. $\delta\mathbf{K}$ is the variation of the stiffness matrix, where it is assumed that the damage effects only the structure stiffness while its mass remains unmodified. The matrix $\delta\mathbf{A}$ is decomposed by a singular value decomposition where the rank of the matrix $\delta\mathbf{A}$ is related to the rank of the matrix $\delta\mathbf{K}$ that gives $\delta\mathbf{K} = \mathbf{U}\mathbf{\Sigma}\mathbf{V}$. By defining the *fault direction matrix*, $\mathbf{F}$, and *failure amplitude*, μ as

$$\mathbf{F} = \begin{Bmatrix} \mathbf{0} \\ -\mathbf{M}^{-1}\mathbf{U} \end{Bmatrix}, \quad \mu = \{\mathbf{\Sigma}\mathbf{V}\ \mathbf{0}\}\,\zeta$$

with ζ being the state vector, the state variable description of the damaged structure can be written as:

$$\dot{\zeta}(t) = \mathbf{A}\zeta(t) + \mathbf{B}\Delta\phi_A + \mathbf{F}\mu, \quad \Delta\phi_S = \mathbf{C}\zeta(t)\,. \quad (11)$$

This procedure can be repeated for each fault location. In (Liberatore, 2002) the first two singular values of the $\delta\mathbf{K}$ matrix are obtained at a fixed damage position and for different damage sizes. The magnitude of the greatest singular value is approximately constant damage sizes, while the magnitude of the others drops sharply with the decrease of fault size. Therefore, only the vector associated with the greatest singular value was chosen as fault direction vector. The variation of *directions* for the fault vectors as function of the damage size was also investigated (Liberatore, 2002) and shown to be invariant. Any sufficiently small damage sizes produces only one significant fault direction vector whose amplitude and direction is approximately independent from fault size, and only dependent on fault location.

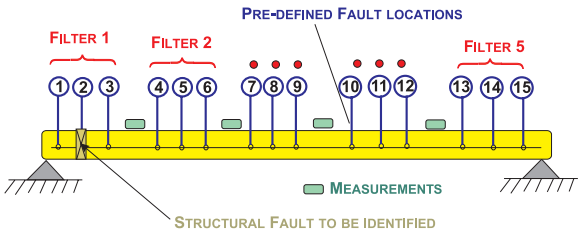

Fig. 3. Scheme of the simply supported beam with 4 measurements and 15 simulated faults used in the design of 5 fault detection filters.

Therefore, one fault vector is associated with each of the fault locations on the beam.

3.3 Filter Design: Detection and Complementary Spaces

The filter design is implemented by defining a set of fault locations evenly spaced over the beam. The number of locations are assumed to be dense enough to approximately identify the damage location. If the number of measurements are half of the dimension of the state vector, then the dimension of the detection space is equal to the dimension of the state space. However, for practical implementations fewer measurements then the number of fault directions are considered. The algorithm applied to the experimental beam uses four measurements and requires five detection filters, each utilizing three pre-defined fault direction vectors. A scheme of the adopted configuration is shown in Figure 3.

The pre-defined fault direction vectors obtained with the procedure described in section 3.2 satisfy the conditions for unique detection and identification of a fault (see reference (White and Speyer, 1987; Douglas and Speyer, 1996)). The detection space is obtained by assigning 6 eigenvalues for all the fault direction filters (improved robustness was obtained by choosing the same two for each detection space), while the complementary space is obtained by assigning additional 22 eigenvalues. In this design procedure, the sets of eigenvalues chosen were complex conjugates and equal for each filter. The complementary subspace is spanned by an arbitrary set of eigenvectors. These additional degrees of freedom along with the choice of eigenvalues are used to enhance filter robustness. The procedure for establishing the detection spaces and the complementary space is described in detail in (Liberatore, 2002).

4. EXPERIMENTAL RESULTS

The experimental setup of the aluminum simply supported beam is shown in Figure 4 while the beam and piezoelectric transducers material

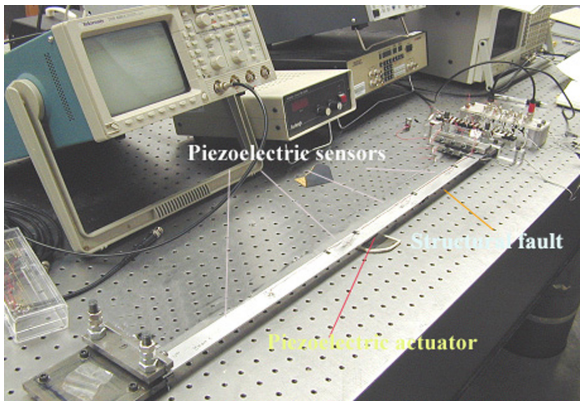

Fig. 4. Experimentaltest setup.

properties and dimensions are listed in Table (1) where $t \sim$ thickness, $b \sim$ width, and $L \sim$ length. Also, the piezoelectric stress/charge coefficient is $d_{31} = -274 \cdot 10^{-12} C/N$ and *clamped* piezoelectric permittivity is $\varepsilon^{SL} = 2.46310^{-8}\ C/Nm^2$.

Table 1. Dimension and material properties

Beam	Sensor and Actuator
$t_B = 3.2\ mm$	$t_S = 0.125\ mm, t_A = 0.6\ mm$
$b_B = 27.5\ mm$	$b_S \equiv b_A = 2.5\ mm$
$L = 0.771\ m$	$L_S \equiv L_A = 4\ mm$
$E_B = 68.9\ GPa$	$E_S = 40.0\ GPa,\ E_A = 80.0\ GPa$
$\rho_B = 2730\ kg/m^3$	$\rho_S \equiv \rho_A = 7750\ kg/m^3$

The piezoelectric sensors are positioned on top of beam surface along the longitudinal midline at 180 mm, 333 mm, 486 mm and 639 mm, respectively, from the left-hand edge of the beam and the piezoelectric actuator is positioned on the bottom surface, along the beam midline, at 397 mm from the left-hand edge of the beam. The choice of sensors and actuator position was decided based on simulation so that both observability and controllability of resulting state-space system was guaranteed. The measured frequency response of the structure from sensor 1 is shown in Figure 5 and is compared with the analytical transfer function obtained from the model. The range of frequency shown in the figure includes the first 14 natural frequencies. The transfer function is obtained with a Stanford Research System Spectrum Analyzer, Model SR785 with 2048 points. The model provides a very good agreement with the measured data with errors in the peak frequencies approximately of the order of 2%, (Liberatore, 2002).

Additional equipment was utilized for the experimental setup: 1) A Wavetek 10 MHz DDs Mod. 29 function generator to produce the sinusoidal inputs for the actuator, 2) a low impedance Burleigh PZ 150 M volt amplifier for the amplification of the actuator input, and 3) a National Instruments PCI-MIO-16E-1 PC card for data acquisition. The data from the sensors and actuator were sampled at 40 K sample/sec and each acquisition lasted

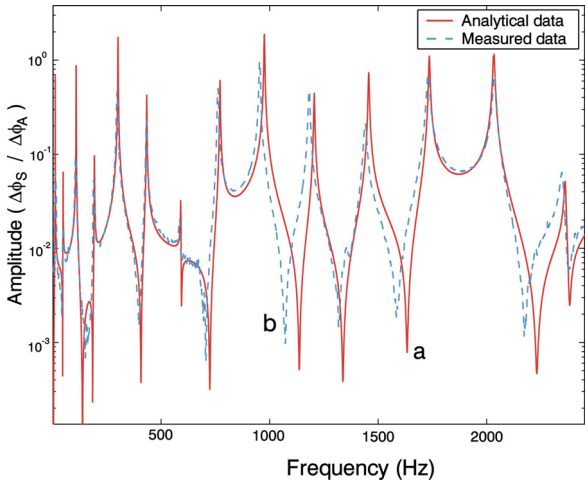

Fig. 5. Input-output frequency response from actuator and sensor 1 of the simply supported beam. a) Analytical versus b) measured data.

approximately 10 seconds. In order to reduce the noise effect, digital Chebychev low pass and band-pass filters were appositely designed for each of the input and output signals. The state integration was obtained with a Runge–Kutta fourth order method using Matlab software. The actuator input was approximately 120 Volts after amplification and the average output from the sensors was approximately 2 Volts [3], The norms of the projected residuals obtained from the undamaged structure had magnitude of approximately 10^{-2}, indicating good tracking of the filter.

The damage inflicted upon the structure was in the form of a saw cut of approximately 5 mm × 1 mm made on one side of the beam at approximately 448 mm from the beam left-hand edge. The saw cut position was chosen coincident with the pre-defined fault location N.9, that is in the set of pre-defined fault direction vectors of filter N.1. After damage, new set of data was taken and compared with the estimate of the fault detection filter. The resulting norms of the projected residuals are shown in Figure 6 for filter N.1, that experience the damage, and for filter N.4, respectively. In the figure, for each filter, in case A) are shown the normalized norm of residuals before damage occurs and in case B) are shown the normalized norms of residuals after damage has occurred. The residuals are normalized with respect to values obtained previously damage had occurred. As it can be seen, in both filters, when there was no damage, all the three residuals had similar values. After damage occurred, in filter N.1, the norm of the pre-defined fault direction, location 9, increased approximately 3 times while

[3] The average measured capacitance of each sensor is $C \cong 3nF$ resulting in high impedance and thereby high voltage outputs even with small currents generally experienced with piezoelectric transducers.

the other two norms, location 13 and 15, were essentially unchanged. This indicated that the projector 9 detected a damage coincident with the fault location 9. For filter N.4, instead, after damage occurred, all the residual norms increased approximately the same amount indicating that no specific fault was detected. Although not shown, the residual norms of filter N.2, 3 and 5, after damage occurred, showed a behavior similar to the one seen for filter N.4 indicating that no specific fault was detected. Therefore, the data shows that damage was coincident with the pre-defined fault location 9. However, for an in-situ health monitoring system, the procedure should include a residual processor so that a probabilistic decision can be made about the structure's health (Malladi and Speyer, 1999).

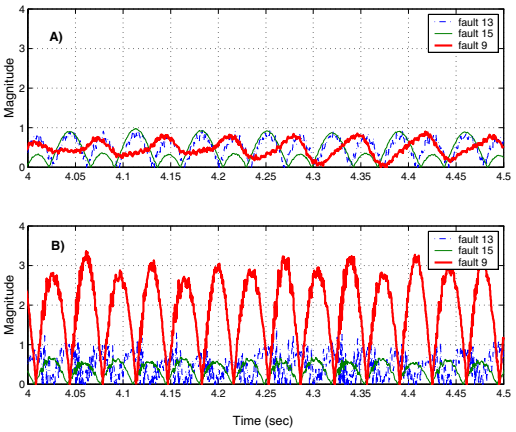

Filter N.1

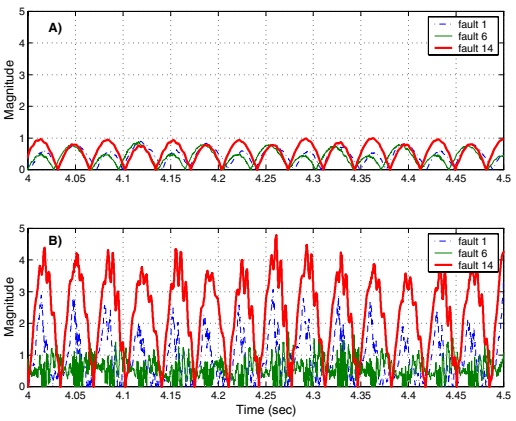

Filter N.2

Fig. 6. Measured data. Filter N.1 and Filter N.4. Normalized norms of the projected residuals: A) Before damage and B) after damage

5. CONCLUSIONS

A bank of fault detection filters were designed for the structural health monitoring of a simply supported beam. The fault direction vectors were obtained by introducing a damaged region in the structure analytical model and upon singular value decomposition of a damaged stiffness matrix. The structural damage was detected and localized in the experimental data obtained from a simply supported aluminum beam. In particular, from measured data, a saw cut of approximately 5 mm × 1 mm made on one side of the beam was detected and localized. In addition, to structural damage, the filter design can also include actuator and sensor fault.

REFERENCES

Beard, R.V. (1971). Failure Accomodation in Linear System through Self-Reorganization. PhD thesis. Massachussets Institute of Technology.

Douglas, R.K. and J.L. Speyer (1996). Robust fault detection filter design. *AIAA Journal of Guidance, Control and Dynamics* **19**(1), 214–218.

Douglas, R.K. and J.L. Speyer (1999). h_∞ bounded fault detection filter. *AIAA Journal of Guidance, Control and Dynamics* **22**(1), 129–138.

Gatti, P.L. and V. Ferrari (1999). *Applied Structural and Mechanical Vibrations: Theory, Methods and Measuring Instrumentation*. E & FN Spon, Taylor and Francis Group. London.

Géradin, M. and D. Rixen (1997). *Mechanical Vibrations—Theory and application to structural dynamics*. 2nd ed.. John Wiley & Sons. New York.

Jones, H.L. (1973). Failure Detection in Linear Systems. PhD thesis. Massachussets Institute of Technology.

Liberatore, S. (2002). Analytical redundancy, fault detection and health monitoring for structures. PhD thesis. University of California, Los Angeles.

Malladi, Durga P. and Jason L. Speyer (1999). A generalized shiryayev sequential probability ratio test for change detection and isolation. *IEEE Transactions on Automatic Control* **AC-44**(8), 1522–1534.

Massoumnia, M-A. (1986). A geometric approach to the synthesis of failure detection filters. *IEEE Transactions on Automatic Control* **AC-31**(9), 839–846.

Parton, V.Z. and B.A. Kudryavtsev (1988). *Electromagnetoelasticity*. Gordon and Breach Science Publisher. New York.

White, J.E. and J.L. Speyer (1987). Detection filter design: Spectral theory and algorithms. *IEEE Transactions on Automatic Control* **AC-32**(7), 593–603.